UCSF
UC San Francisco Previously Published Works

Title

RNAi screen identifies a role for adaptor protein AP-3 in sorting to the regulated secretory pathway

Permalink

https://escholarship.org/uc/item/2dv7x3dt

Journal

Journal of Cell Biology, 191(6)

ISSN

0021-9525

Authors

Asensio, Cédric S
Sirkis, Daniel W
Edwards, Robert H

Publication Date

2010-12-13

DOI

10.1083/jcb.201006131

Copyright Information

This work is made available under the terms of a Creative Commons Attribution-NonCommercial-ShareAlike License, available at https://creativecommons.org/licenses/by-nc-sa/4.0/

Peer reviewed

eScholarship.org Powered by the California Digital Library
University of California

THE JOURNAL OF CELL BIOLOGY

RNAi screen identifies a role for adaptor protein AP-3 in sorting to the regulated secretory pathway

Cédric S. Asensio,[1,2] Daniel W. Sirkis,[1,2,3] and Robert H. Edwards[1,2,3]

[1]Department of Physiology, [2]Department of Neurology, and [3]Graduate Programs in Pharmacogenomics and Cell Biology, University of California, San Francisco, San Francisco, CA 94158

The regulated release of proteins depends on their inclusion within large dense-core vesicles (LDCVs) capable of regulated exocytosis. LDCVs form at the trans-Golgi network (TGN), but the mechanism for protein sorting to this regulated secretory pathway (RSP) and the cytosolic machinery involved in this process have remained poorly understood. Using an RNA interference screen in *Drosophila melanogaster* S2 cells, we now identify a small number of genes, including several subunits of the heterotetrameric adaptor protein AP-3, which are required for sorting to the RSP. In mammalian neuroendocrine cells, loss of AP-3 dysregulates exocytosis due to a primary defect in LDCV formation. Previous work implicated AP-3 in the endocytic pathway, but we find that AP-3 promotes sorting to the RSP within the biosynthetic pathway at the level of the TGN. Although vesicles with a dense core still form in the absence of AP-3, they contain substantially less synaptotagmin 1, indicating that AP-3 concentrates the proteins required for regulated exocytosis.

Introduction

The function of proteins involved in extracellular signaling depends on their regulated secretion in response to the appropriate stimuli. Regulated secretion contributes to the roles of peptide hormones such as insulin, neural peptides such as opioids, and growth factors such as brain-derived neurotrophic factor. Thus, the regulated release of proteins has a central role in human disease and normal physiology, synaptic plasticity, behavior, and development.

The regulated secretion of proteins requires their sorting into a specialized secretory pathway capable of regulated exocytosis, the regulated secretory pathway (RSP). In contrast to the constitutive secretory pathway, which confers the immediate release of newly synthesized proteins from essentially all eukaryotic cells, the RSP enables release from specialized cells in response to physiologically appropriate signals. However, we know very little about how proteins sort into the regulated rather than the constitutive pathway.

Morphologically, the RSP usually corresponds to large vesicles containing a dense core of aggregated cargo. These large dense-core vesicles (LDCVs) bud from the TGN (Orci et al., 1987; Tooze and Huttner, 1990; Eaton et al., 2000), and lumenal interactions such as the aggregation of granulogenic proteins have been suggested to drive their formation (Kim et al., 2001; Turkewitz, 2004). Previous work has also suggested that sorting to LDCVs occurs by default, with proteins destined for other organelles removed during the subsequent, well-established process of LDCV maturation (Arvan and Castle, 1998; Morvan and Tooze, 2008). However, the direct analysis of budding from the TGN has demonstrated the sorting of regulated from constitutive cargo at this step, before maturation (Tooze and Huttner, 1990). LDCV membrane proteins such as carboxypeptidase E and sortilin may serve as the receptors for soluble cargo (Cool et al., 1997; Chen et al., 2005). In contrast to these lumenal interactions, we know little about any cytosolic machinery like those that generate transport vesicles from essentially all of the other membrane compartments in eukaryotic cells.

Several membrane proteins contain cytosolic sequences that direct them to LDCVs. In the case of the enzyme peptidylglycine α-amidating monooxygenase and the endothelial adhesion molecule P-selectin, however, these sequences are not

Correspondence to Robert H. Edwards: robert.edwards@ucsf.edu

Abbreviations used in this paper: ANF, atrial natriuretic factor; dsRNA, double-stranded RNA; dVMAT, *Drosophila* VMAT; HSPG, heparan sulfate proteoglycan; LDCV, large dense-core vesicle; LPS, lipopolysaccharide; LRO, lysosome-related organelles; PP1, protein phosphatase 1; RSP, regulated secretory pathway; ss, signal sequence; TIRF, total internal reflection fluorescence; VMAT, vesicular monoamine transporter; wt, wild type.

© 2010 Asensio et al. This article is distributed under the terms of an Attribution–Noncommercial–Share Alike–No Mirror Sites license for the first six months after the publication date (see http://www.rupress.org/terms). After six months it is available under a Creative Commons License (Attribution–Noncommercial–Share Alike 3.0 Unported license, as described at http://creativecommons.org/licenses/by-nc-sa/3.0/).

The Rockefeller University Press $30.00
J. Cell Biol. Vol. 191 No. 6 1173–1187
www.jcb.org/cgi/doi/10.1083/jcb.201006131

required for sorting to the RSP because lumenal interactions suffice (Blagoveshchenskaya et al., 2002; Harrison-Lavoie et al., 2006). However, the neuronal vesicular monoamine transporter 2 (VMAT2), which fills LDCVs and synaptic vesicles with monoamines, depends on a conserved C-terminal cytoplasmic dileucine-like motif (K*EE*KMA**IL**) for sorting to LDCVs (Liu et al., 1994; Erickson et al., 1995). Mutation of the dileucine-like core (bold letters) disrupts multiple trafficking events including endocytosis, but replacement of the upstream acidic residues (Glu-478 and -479 [italic letters above]) with alanine (EE/AA mutation) diverts VMAT2 from the regulated to the constitutive secretory pathway, increasing cell surface delivery without affecting endocytosis (Krantz et al., 1997). Glu-478 and -479 thus appear to have a specific role in sorting to the RSP, and the LDCV membrane protein phogrin contains a remarkably similar sequence also required for localization to LDCVs (Torii et al., 2005). Because VMAT2 does not appear at the cell surface before sorting to LDCVs (Li et al., 2005), the motif presumably acts within the biosynthetic rather than endocytic pathway, most likely at the level of the TGN, where LDCVs form. The requirement for a cytoplasmic motif in sorting to the RSP further suggests an interaction with cytosolic sorting machinery. Indeed, we have now used VMAT as a reporter to identify genes involved in biogenesis of the RSP.

Results

The increased plasma membrane expression of EE/AA VMAT2 caused by its diversion from the regulated to constitutive secretory pathway (Krantz et al., 2000) suggested that cellular defects in sorting to the RSP might similarly increase the surface delivery of wild-type (wt) VMAT2. We have thus used the cell surface exposure of VMAT to screen for genes involved in biogenesis of the RSP. Although endocytosis might be expected to influence cell surface expression, direct sorting of VMAT2 to the RSP at the level of the TGN, without passage through the plasma membrane (Li et al., 2005), should minimize the chance of identifying genes involved in endocytosis. Screening for increased surface delivery should also reduce the likelihood of identifying genes with nonspecific deleterious effects.

Drosophila melanogaster S2 cells exhibit an RSP

Drosophila S2 cells are very sensitive to RNAi and have been used to screen for genes involved in a wide range of cellular processes (Foley and O'Farrell, 2004; Bard et al., 2006; Goshima et al., 2007; Guo et al., 2008), but it is not known whether S2 cells express sorting machinery that can recognize the dileucine-like motif in VMAT. However, even constitutive secretory cells such as Chinese hamster ovary cells have been suggested to express a cryptic pathway for regulated secretion (Chavez et al., 1996). To test this possibility in S2 cells, we used *Drosophila* VMAT (dVMAT), which contains a dileucine-like motif (S*DE*KKS**LI**) remarkably similar to the mammalian sequence, with two acidic residues (italics) 4 and 5 positions upstream of the dileucine (bold; Greer et al., 2005). We replaced the upstream acidic residues (Asp-584 and Glu-585) with alanine (DE/AA mutation) using a lumenal HA epitope tag to assess surface expression (Greer et al., 2005) and a fusion of GFP to the N terminus of dVMAT to determine the total amount of protein expressed. S2 cells were incubated for 2 h with HA antibody conjugated to Alexa Fluor 647, and flow cytometry was used to quantify the fluorescence of individual cells. Despite equivalent total dVMAT expression, we observed very low cell surface delivery of wt dVMAT relative to the DE/AA mutant. A scatter plot shows that DE/AA dVMAT has a much higher ratio of Alexa Fluor 647 to GFP fluorescence than wt (Fig. 1 A), with an approximately sevenfold difference in mean surface/total transporter, and $P < 10^{-14}$ by Kolmogorov-Smirnov analysis of the cumulative frequency distribution for ratios from individual cells (Fig. 1 B). Because the analogous mutation in rat VMAT2 has a very similar effect on cell surface expression and selectively disrupts sorting to the RSP (Krantz et al., 1997; Li et al., 2005), we infer that S2 cells must express some of the same sorting machinery.

We then determined whether S2 cells can in fact mediate regulated secretion using a fusion of GFP to mammalian atrial natriuretic factor (ANF) because this peptide hormone has been shown to undergo regulated exocytosis in *Drosophila* (Shakiryanova et al., 2005). As control, we fused GFP directly to the signal sequence (ss) of ANF. Measurement of fluorescence in the supernatant shows an approximately fivefold less basal secretion of ANF-GFP than ss-GFP even after normalization to total GFP expression (Fig. 1 C), indicating efficient storage of ANF. To determine whether S2 cells can release ANF in a regulated manner, we stimulated cells expressing ANF-GFP for 1 h with lipopolysaccharide (LPS). LPS increases secretion of ANF-GFP by about twofold (Fig. 1 D), and this effect is blocked by the removal of external Ca^{2+} (Fig. 1 E). LPS also has no effect on secretion of ss-GFP (Fig. 1 D), which is consistent with the constitutive release of this protein. In addition, because LDCVs differ from other secretory vesicles in their dependence on the calcium-dependent activator protein for secretion (Martin and Walent, 1989; Berwin et al., 1998; Elhamdani et al., 1999; Speese et al., 2007), we used double-stranded RNA (dsRNA) to knock down the *Drosophila* orthologue and found that this eliminates regulated release of ANF from S2 cells (Fig. 1 F). S2 cells thus express a functional RSP. Colocalization of mCherry-dVMAT with ANF-GFP but not ss-GFP (Fig. S1) further supports the sorting of dVMAT to this pathway.

An RNAi screen in S2 cells identifies genes that regulate cell surface dVMAT expression

To identify cellular machinery involved in biogenesis of the RSP, we performed a genome-wide RNAi screen in S2 cells using a library of 7,216 sequences that target *Drosophila* genes conserved to mammals. S2 cells transfected with GFP-dVMAT-HA were seeded into 96-well plates and treated twice with dsRNA. After treatment for 6 d, the cells were incubated with HA antibody conjugated to Alexa Fluor 647 and assayed for antibody uptake and total expression by high-throughput flow cytometry, enabling individual measurements from many cells for each condition (Fig. 2 A). The ratio of surface/total dVMAT was computed for

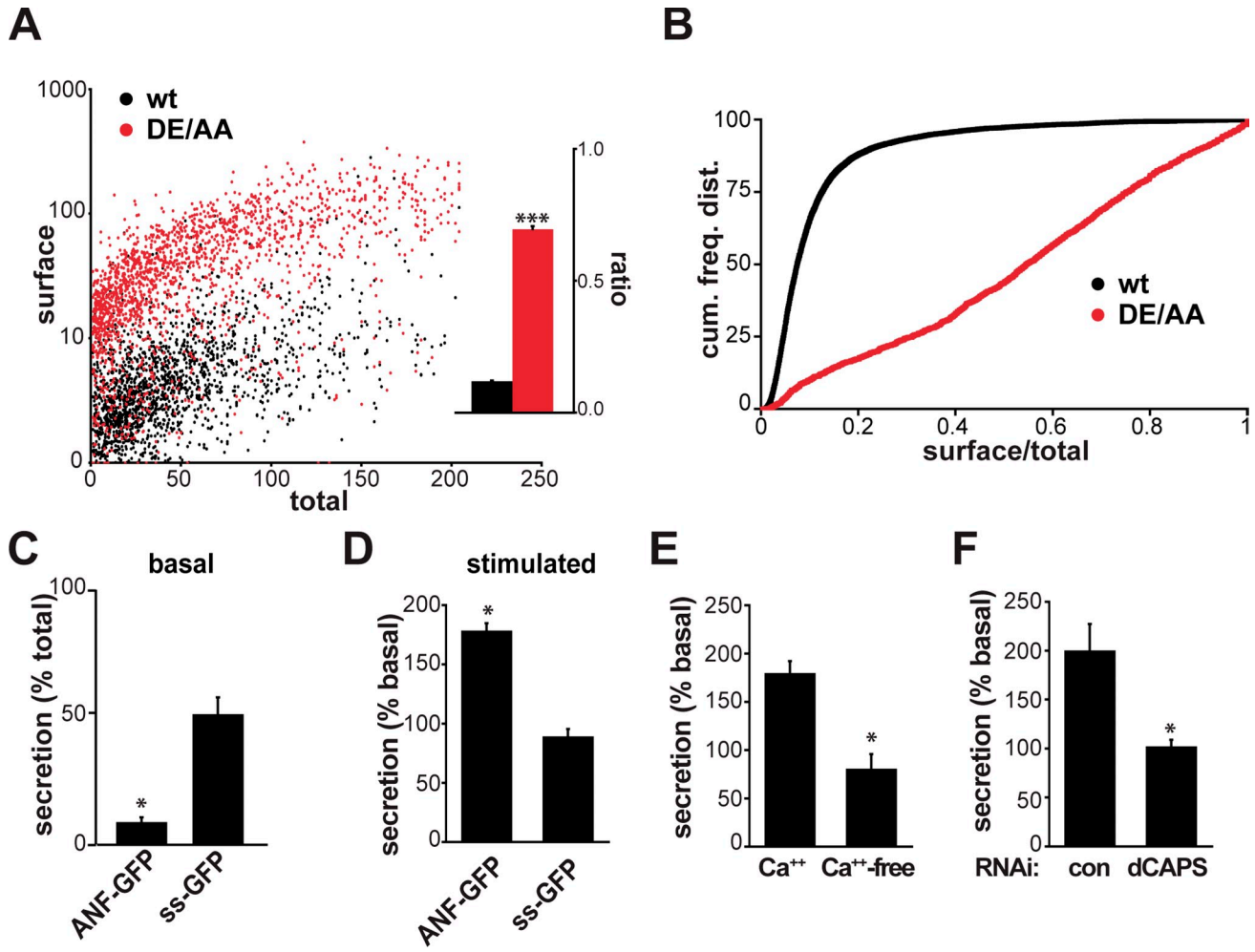

Figure 1. **S2 cells express an RSP.** (A and B) S2 cells were transiently transfected with wt (black) or DE/AA (red) GFP- and HA-tagged dVMAT, incubated for 2 h at room temperature with external HA antibody conjugated to Alexa Fluor 647, washed, and the fluorescence of individual cells was determined by flow cytometry (A). (inset) The bar graph displays the mean ratio of surface/total fluorescence (n > 1,800 cells). Kolmogorov-Smirnov analysis of the cumulative frequency distributions binned by surface/total dVMAT ratios (B) indicates a significant change in the DE/AA distribution relative to wt (***, $P < 10^{-14}$). (C–F) S2 cells were transiently transfected with ANF-GFP (C–E) or the signal sequence of ANF fused directly to GFP (ss-GFP; C and D), washed, incubated for 1 h, and the cellular and secreted GFP fluorescence were measured using a plate reader. (C) Normalized to intracellular fluorescence, the media of cells expressing ANF-GFP shows less fluorescence than cells expressing ss-GFP. (D) Treatment with 100 µg/ml LPS induces secretion of ANF-GFP but not ss-GFP. (E and F) Pretreatment with BAPTA-AM in calcium-free buffer (E) or knockdown of *Drosophila* calcium-dependent activator protein for secretion (dCAPS) with dsRNA (F) block the secretion evoked by LPS. *, $P < 0.05$ by two-tailed Student's t test. The data represent mean values from three to four independent experiments, and error bars indicate SEM.

each cell, and a z score was calculated relative to other wells in the same plate as controls. The entire screen was performed twice, once using transiently transfected S2 cells and a second time with stable transformants. After removing genes that reduced the number of cells available for analysis or that influenced expression of the GFP-tagged reporter (Table S1), we focused on the remaining positives from both screens with z score ≥3. Because essentially all of the excluded genes affect transcription or translation, we excluded a small number of additional sequences because they also involve transcription or translation.

We retested the remaining 18 genes with nonoverlapping dsRNA sequences to exclude false positives caused by off-target effects. In at least two of four independently performed experiments, we confirmed the increase in dVMAT surface expression for 16 of the 18 genes ($P < 0.003$ by Kolmogorov-Smirnov analysis of the cumulative frequency distributions; Fig. 3). Remarkably, the screen identified nine proteins with a primary role in membrane trafficking, including four cytoskeletal proteins or enzymes implicated in the regulation of membrane trafficking, and two proteins of unknown function (Table I). Because the genes identified may influence VMAT surface expression through a variety of mechanisms, including some unrelated to the RSP, we then performed a series of secondary screens.

Dependence on the VMAT sorting motif

To determine whether the effect of genes identified in the screen depends on the VMAT dileucine-like motif, we examined their interaction with the DE/AA mutation. Class I genes increase HA antibody uptake by DE/AA and wt dVMAT (Fig. 3, top), suggesting that they act independently of the extended dileucine. Mechanisms that might account for the additive effect include an impairment of endocytosis and an increase in constitutive secretion.

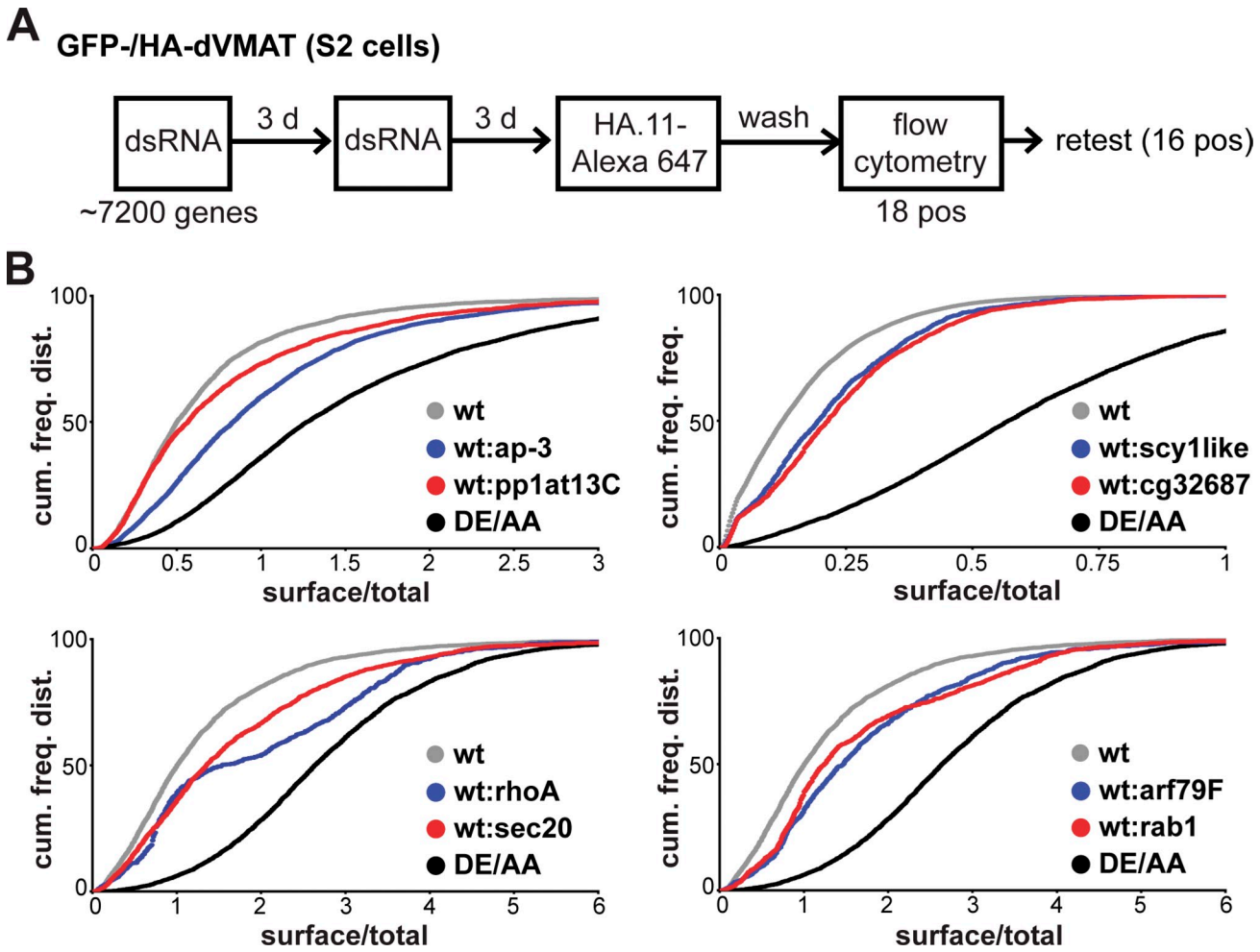

Figure 2. **S2 cell screen identifies genes that regulate the surface expression of dVMAT.** (A) The flow chart illustrates the procedure used for screening. S2 cells transfected with GFP-/HA-dVMAT were treated twice with dsRNA over a 6-d period in a 96-well plate, incubated with external HA antibody conjugated to Alexa Fluor 647 for 2 h, washed, and the fluorescence of both GFP and Alexa Fluor 647 was measured at the level of individual cells by flow cytometry. Of 7,200 genes conserved from *Drosophila* to mammals, 18 positives (z score ≥ 3) were identified and retested using nonoverlapping dsRNA. Kolmogorov-Smirnov analysis of the cumulative frequency distribution reveals that 16 of 18 genes were again positive ($P < 0.005$ in at least two independent experiments). (B) Cumulative frequency distributions for selected dsRNA in representative retest experiments show the differences from control (wt) and DE/AA dVMAT.

Indeed, we identified the μ subunit of adaptor protein AP-2 (μ2) presumably because it has an important role in clathrin-dependent endocytosis, and knockdown would be expected to increase cell surface expression of DE/AA dVMAT because the mutant resides at higher levels than wt at the plasma membrane. It is more surprising that knockdown of AP-2 increases HA antibody uptake by wt dVMAT considering the low rate of its delivery to the plasma membrane, but we did not identify other proteins known to be involved in endocytosis. To determine whether the knockdown of other class I genes increases cell surface dVMAT by promoting constitutive secretion, we examined the basal release over 1 h of ANF-GFP from unstimulated S2 cells. dsRNA to the catalytic subunit of protein phosphatase 1 (PP1), sec20, and particularly rhoC all significantly increased release of ANF-GFP (Fig. 3, top middle), and the role of sec20 in retrograde transport from Golgi to endoplasmic reticulum presumably accounts for the effect of dsRNA to this gene (Lewis et al., 1997).

Knockdown of class II genes (*rab1*, *arf79F*, and *cg32687*) reduces HA antibody uptake by DE/AA dVMAT (Fig. 3, middle). Because dsRNA to these sequences increases antibody uptake by wt dVMAT, an opposite effect on the mutant might appear surprising. However, the discrepancy may simply reflect a role for these proteins in constitutive and regulated secretion, with targeting to the constitutive pathway making DE/AA dVMAT more sensitive than wt to the RNAi. Consistent with this possibility and partial knockdown by the dsRNA, complete block of the secretory pathway with brefeldin A significantly reduces DE/AA dVMAT surface expression without any discernible effect on the low surface levels of wt dVMAT (unpublished data). In addition, a screen for genes important in constitutive secretion has already identified *rab1* and *arf79F* (homologous to Arf1 in mammals; Bard et al., 2006), and we find that their knockdown decreases constitutive secretion of ANF-GFP (Fig. 3, middle). Class II genes may thus have roles in both regulated and constitutive pathways.

Class III genes show no additional effects on HA antibody uptake by DE/AA dVMAT (Fig. 3, bottom), suggesting their

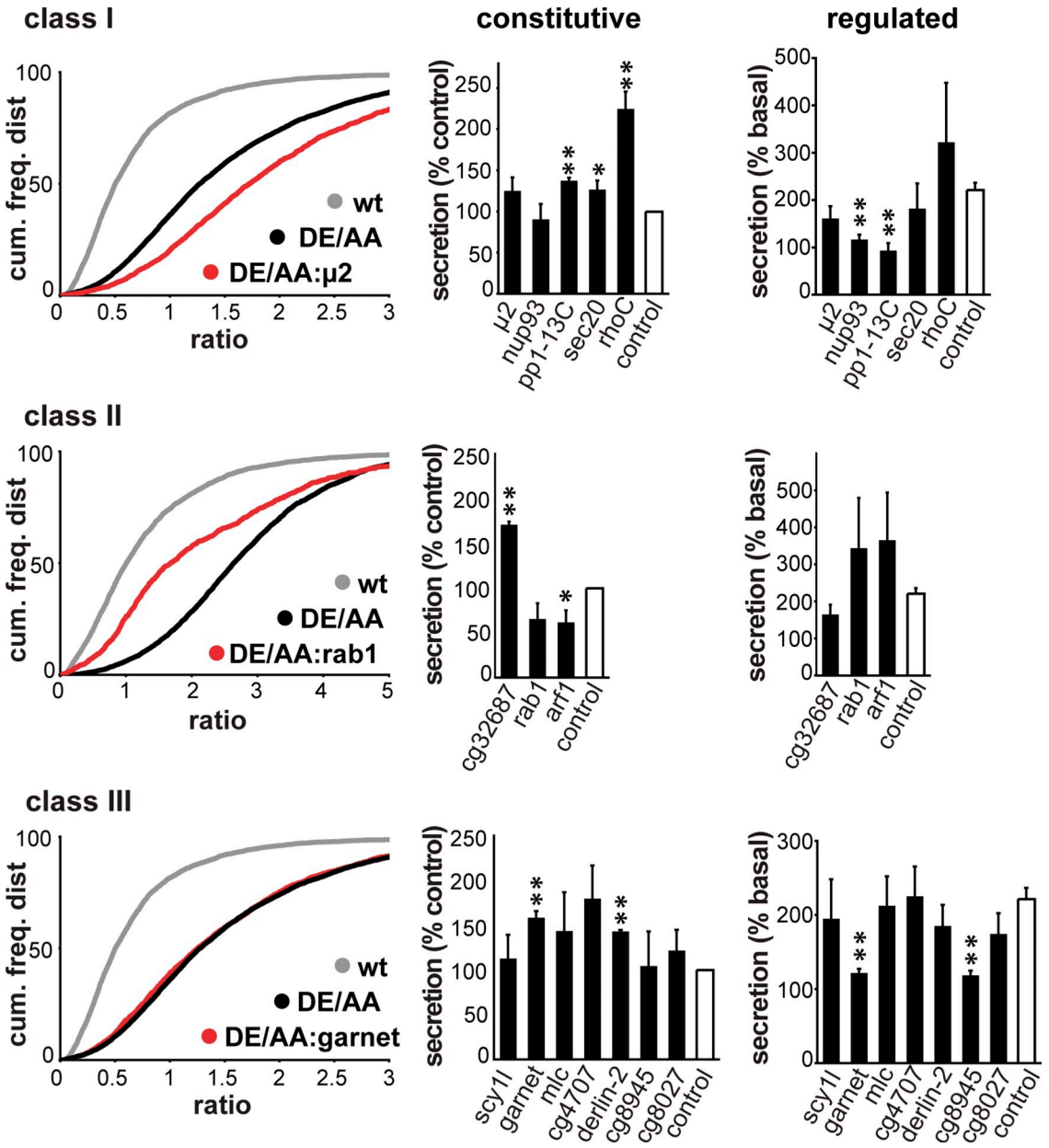

Figure 3. **Classification of genes identified in the screen by mechanism and effect on the regulated secretion of soluble cargo.** S2 cells transfected with DE/AA GFP-/HA-dVMAT were treated with dsRNA-targeting genes identified in the screen, and the uptake of external HA antibody was measured as described in Fig. 1. (left) Representative cumulative frequency distributions are shown for selected genes in each class. Class I genes increase, class II genes decrease, and class III genes have no effect on antibody uptake by DE/AA dVMAT. (middle) S2 cells expressing ANF-GFP were treated with dsRNA and basal (unstimulated) secretion of GFP fluorescence determined as in Fig. 1 C. Secretion was normalized to cellular ANF-GFP and expressed as a percentage of the fluorescence secreted by control cells. (right) S2 cells expressing ANF-GFP were treated with dsRNA and LPS-induced secretion measured as in Fig. 1 D. *, $P < 0.05$; **, $P < 0.01$ (relative to control by two-tailed Student's *t* test; $n = 3–5$). The data show mean values, and error bars indicate SEM.

dependence on the extended dileucine motif. Indeed, Scy1-like kinase and *N*-acetylglucosamine (GlcNAc)–1-phosphotransferase have been implicated in trafficking through the Golgi complex, back to the endoplasmic reticulum and to lysosomes, respectively (Tiede et al., 2005; Burman et al., 2008). However, RNAi to Scy1-like kinase or GlcNAc-1-phosphotransferase does not increase constitutive release of ANF-GFP (Fig. 3, bottom middle). In contrast, two other dsRNAs in this class (*garnet* and *derlin*) increase the constitutive release of ANF, which is consistent with diversion of this soluble protein from the regulated to the constitutive pathway.

To determine whether genes identified in the screen actually impair the regulated secretion of soluble cargo as well as the sorting of a polytopic membrane protein, we examined the regulated release of ANF-GFP in response to stimulation with LPS. Most of the genes identified do not affect the regulation of release, suggesting either independent effects on cell surface expression of VMAT or differential effects on the sorting of membrane and soluble cargo. However, knockdown of two class I (*nup93* and *pp1-13C*) and two class III genes (*garnet* and *cg8945*) do abolish regulated release (Fig. 3). The screen has thus identified a small number of genes required for regulated secretion.

Table I. **Genes identified in the S2 cell screen and confirmed with nonoverlapping dsRNA**

Cg	Gene symbol	Homologue/domain	Z score	Class
8416	Rho1	RhoC	5.8	I
2023	Cg2023	Sec20	3.6	I
7057	AP-50	AP-2μ1	3.2	I
7262	Cg7262	Nucleoporin 93	3.0	I
9156	PP1-13C	PP1cc	3.0	I
3320	Rab1	Rab1A	3.8	II
8385	Arf79F	Arf1	3.3	II
32687	Cg32687	Leucine-rich repeat 58	3.0	II
11427	Ruby	AP-3β2	3.8	III
11197	Garnet	AP-3∂1	3.7	III
8945	Cg8945	Carboxypeptidase	3.4	III
14899	Cg14899	Derlin-2	3.3	III
3201	Mlc-c	Myosin light chain	3.3	III
4707	Cg4707	Zinc finger	3.1	III
1973	Yata	Scy1-like kinase	3.0	III
8027	Cg8027	GlcNAc-1-phosphotransferase (α^-/β^-)	3.0	III

List of genes identified as positive in the S2 cell screen using GFP-/HA-tagged dVMAT as reporter. The z score indicates significance assessed using a within-plate comparison. Class I dsRNAs increase cell surface expression of DE/AA dVMAT, class II reduce surface expression of the mutant, and class III have no effect.

Loss of AP-3 dysregulates secretion from mammalian neuroendocrine cells

Remarkably, two genes identified in the screen (*garnet* and *ruby*) encode subunits of the heterotetrameric AP-3 complex. The third subunit of AP-3 present in the library (*carmine*) was confirmed positive on specific retesting, and the fourth subunit (*orange*) was not present in the library. AP-3 is known to play a role in the formation of lysosome-related organelles (LROs) such as melanosomes and platelet-dense granules, in addition to synaptic vesicles (Newell-Litwa et al., 2007). Similar to

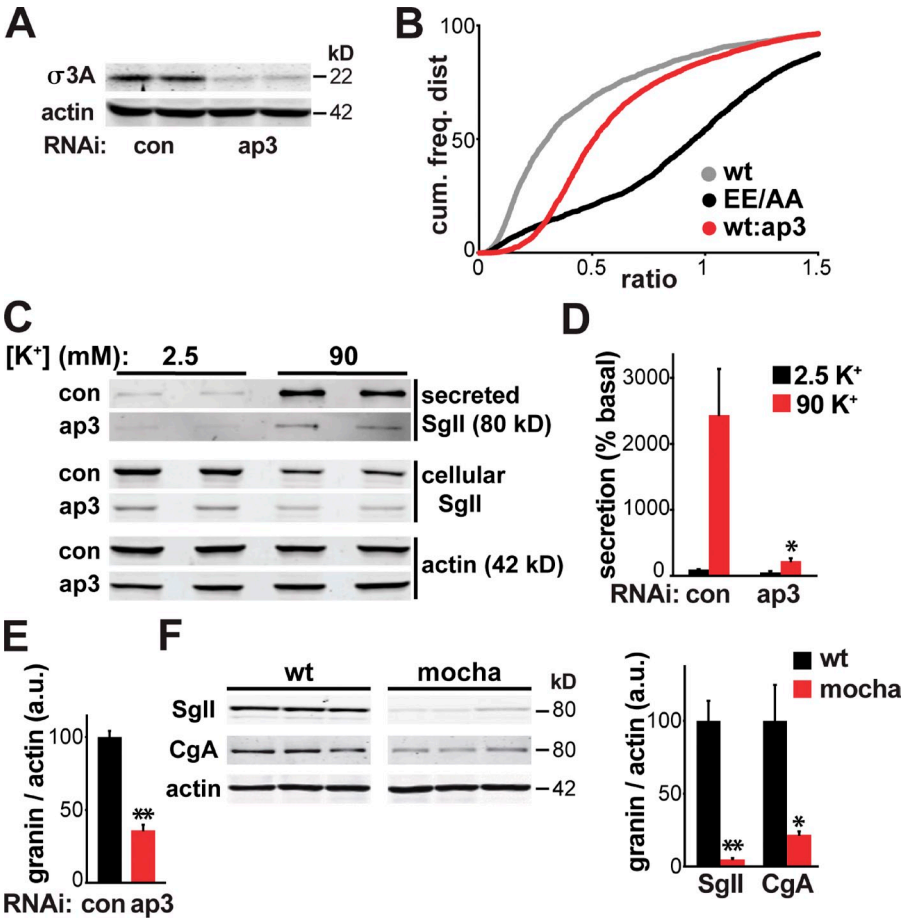

Figure 4. **AP-3 RNAi increases VMAT2 surface expression and impairs regulated release of SgII from PC12 cells.** (A and B) Western analysis of extracts from PC12 cells transiently transfected with 50 nM AP-3 siRNA show an ~80% reduction in AP-3δ subunit σ3A relative to cells transfected with control siRNA (A). PC12 cells cotransfected with wt or EE/AA GFP-/HA-VMAT2 with or without AP-3δ siRNA were subjected to flow cytometry as described in Fig. 1 B. Kolmogorov-Smirnov analysis of the cumulative frequency distributions for wt VMAT2 + control siRNA (gray), wt VMAT2 + AP-3δ siRNA (red), and EE/AA VMAT2 + control siRNA (black) indicates a significant change in the AP-3 siRNA distribution relative to wt ($P < 10^{-14}$). (C and D) PC12 cells were transiently transfected with AP-3δ or control siRNA, washed, and incubated for 30 min in Tyrode's solution containing 2.5 mM (basal) or 90 mM (stimulated) K^+. Cellular and secreted SgII were measured by quantitative fluorescent immunoblotting (C), with the secreted SgII normalized to basal secretion in the control (D). AP-3δ RNAi greatly reduces the depolarization-induced secretion of SgII. *, $P < 0.05$ relative to stimulated secretion from control by two-tailed Student's *t* test ($n = 4$). (E) AP-3δ RNAi reduces the cellular content of SgII relative to actin. *, $P < 0.005$ relative to control by two-tailed Student's *t* test ($n = 4$). (F) The adrenal glands of *mocha* mice lacking AP-3 show a dramatic reduction in the content of SgII and chromogranin A (CgA) relative to the adrenals of control littermates. *, $P < 0.05$; **, $P < 0.005$ (relative to wt by two-tailed Student's *t* test; $n = 3$). The data show mean values, and error bars indicate SEM.

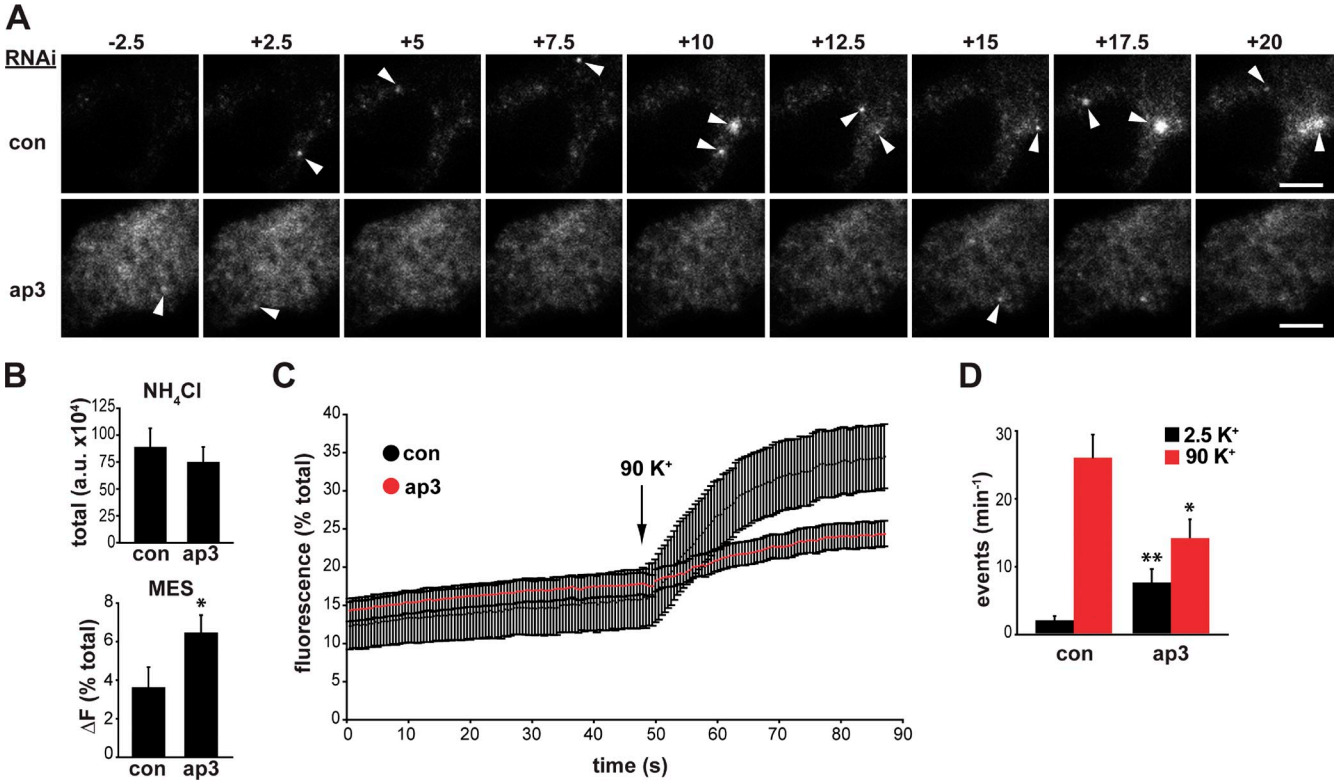

Figure 5. **AP-3 RNAi dysregulates the exocytosis of VMAT2.** PC12 cells were transfected with 50 nM AP-3δ or control siRNA, cotransfected 2 d later with the same siRNA and VMAT2 containing a lumenal pHluorin (VMAT2-pHluorin), then imaged live by TIRF microscopy after an additional 2 d. Basal exocytosis of VMAT2-pHluorin was measured in Tyrode's solution containing 2.5 mM K^+, and release was stimulated in Tyrode's with 90 mM K^+ for 60 s. (A) Representative images acquired before and after depolarization show increased baseline fluorescence and fewer stimulated events (arrowheads) after transfection with AP-3 siRNA (Videos 1 and 2). (B) Total VMAT2 fluorescence was revealed by alkalinization in Tyrode's solution containing 50 mM NH_4Cl, pH 7.4 (top), and surface VMAT2-pHluorin revealed by acidification in Tyrode's with 25 mM MES, pH 6.5 (bottom). AP-3δ RNAi increases the surface fraction of VMAT2 in cells despite expression equivalent to transfection with control siRNA. *, $P < 0.05$ relative to control by two-tailed Student's *t* test ($n = 12$ for control and 14 for AP-3 siRNA). (C) Whole cell fluorescence expressed as a percentage of total fluorescence (revealed in NH_4Cl) shows a robust response to depolarization with 90 mM K^+ (arrow) in control cells but a greatly impaired response after AP-3 siRNA. The traces indicate the mean values of 12 individual traces for control and 14 for AP-3 RNAi cells. (D) The quantification of individual exocytotic events shows increased basal VMAT2-pHluorin exocytosis with AP-3 RNAi but a reduction in stimulated exocytosis. *, $P < 0.02$; **, $P < 0.002$ (relative to control by two-tailed Student's *t* test; control, $n = 31$; AP-3, $n = 19$). Error bars indicate SEM. Bars, 5 µm.

LDCVs, LROs are acidic, and some can undergo regulated exocytosis. However, AP-3 contributes to formation of these organelles from endosomes, whereas LDCVs bud directly from the TGN within the biosynthetic pathway (Tooze and Huttner, 1990; Eaton et al., 2000).

To assess a role for AP-3 in sorting to the LDCVs of mammalian neuroendocrine cells, we used rat pheochromocytoma PC12 cells. Knockdown of the sole AP-3 δ subunit destabilizes the complex (Kantheti et al., 1998), reducing the amount of σ3A by ~80% (Fig. 4 A) and very substantially increasing HA antibody uptake by VMAT2 (Fig. 4 B). In addition, the loss of AP-3 greatly impairs the stimulation of SgII (secretogranin II) release by depolarization, with little effect on the absolute amount of basal release (Fig. 4, C and D). However, because AP-3 knockdown reduces the cellular content of SgII (to ~35% of control cells; Fig. 4 E), constitutive release is in fact increased relative to control, which is consistent with diversion from the regulated to constitutive pathway.

To determine whether the loss of AP-3 has a similar effect on LDCV composition in vivo, we measured the granin content of adrenal glands from *mocha* mice, which lack AP-3. Both SgII and chromogranin A show a dramatic reduction in *mocha* mice (to ~5% and ~20% of wt animals, respectively; Fig. 4 F), which is consistent with the results from PC12 cells, and excluding an off-target effect of the RNAi. Identified in *Drosophila* S2 cells as important for sorting to the RSP, AP-3 thus has a similar role in the regulated exocytosis of both membrane and soluble cargo by mammalian neuroendocrine cells.

A previous study has shown that the loss of AP-3 increases the amount of monoamine released per vesicle and the size of LDCVs, but it did not examine the regulation of release (Grabner et al., 2006). To assess the regulated exocytosis of LDCVs, we used direct, optical imaging of a reporter based on the ecliptic pHluorin (Miesenböck et al., 1998), a modified form of GFP that undergoes quenching at the low pH of secretory vesicles and thus increases in fluorescence with exocytosis (Sankaranarayanan et al., 2000). In particular, we fused the pHluorin to a lumenal domain of VMAT2 (Onoa et al., 2010) and monitored individual exocytotic events at the plasma membrane of live, transfected PC12 cells by total internal reflection fluorescence (TIRF) microscopy. Because the low surface expression of VMAT2-pHluorin complicates identification of the transfected cells, we alkalinized

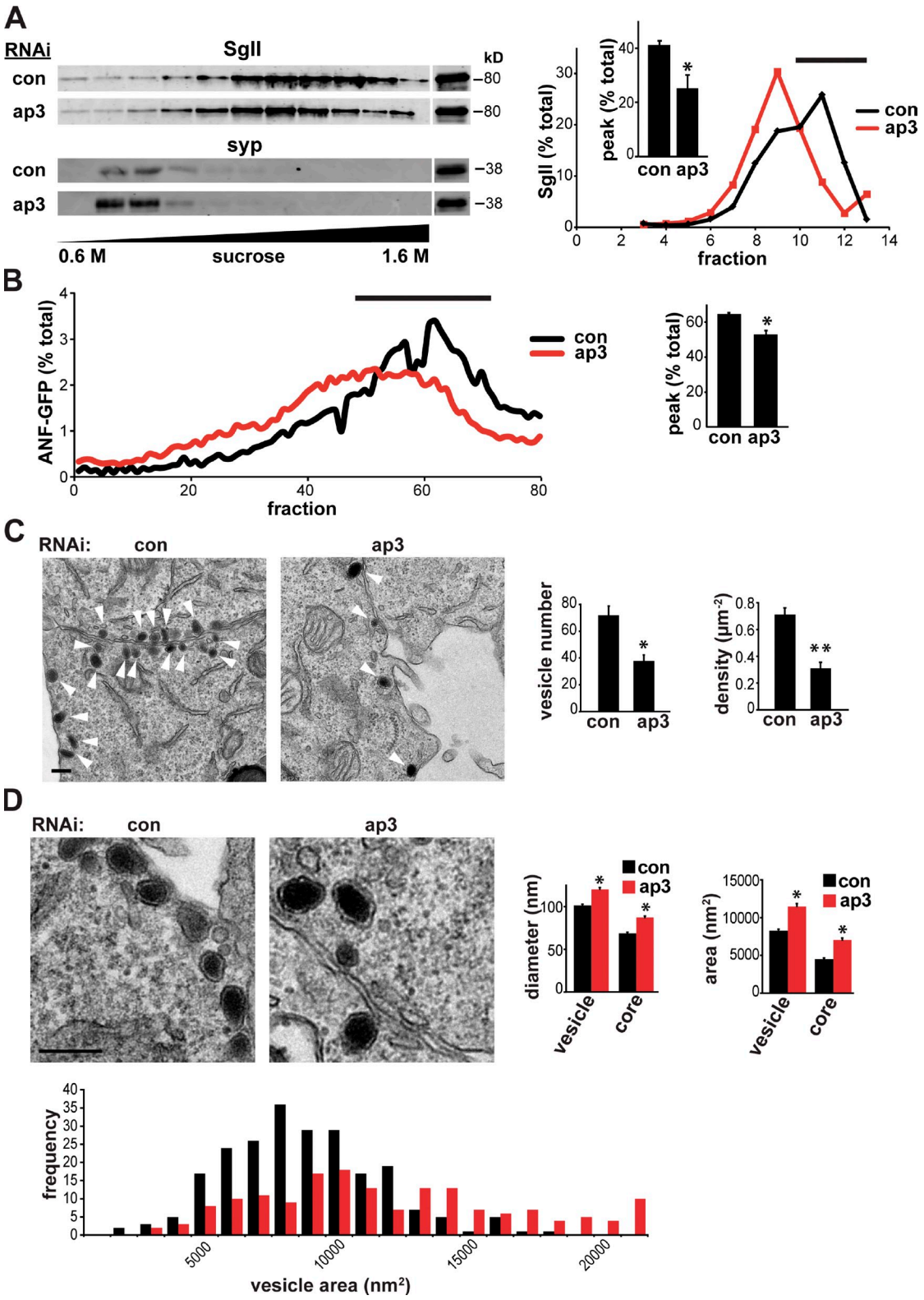

Figure 6. **AP-3 RNAi affects the properties of LDCVs.** (A and B) PC12 cells were transfected twice with 50 nM AP-3δ or control siRNA, and the postnuclear supernatant (input) obtained 2–3 d after the second transfection was separated by equilibrium sedimentation through 0.6–1.6 M sucrose. Fractions were collected from the top of the gradient and assayed for synaptophysin (syp) and SgII by quantitative fluorescent immunoblotting, with each fraction expressed as the percentage of total gradient immunoreactivity, and the area under the LDCV peak (black lines) expressed as a percentage of the area under the entire curve (inset). (A) AP-3 RNAi greatly reduces the LDCV peak and shifts the SgII immunoreactivity toward lighter fractions without affecting the synaptic vesicle protein synaptophysin. *, $P < 0.05$ relative to control by two-tailed Student's *t* test ($n = 3$ transfections). (B) PC12 cells were cotransfected with ANF-GFP and either AP-3 or control siRNA, and the postnuclear supernatant was sedimented as in A. In this case, however, ~80 fractions were collected from the top of the gradient directly into a 96-well plate, and the fluorescence of ANF-GFP was measured directly using a plate reader. The graph indicates ANF-GFP fluorescence for each fraction expressed as a percentage of total gradient fluorescence. (right) The bar graph shows the area under the curve for the LDCV

the internal compartments briefly with NH_4Cl to reveal the total fluorescence and selected cells with similar expression levels (Fig. 5 B). In addition, we briefly lowered the external pH to 5.5, and observed substantially increased quenching of VMAT2-pHluorin after AP-3 knockdown (Fig. 5 B), which is consistent with increased cell surface expression. Cells treated with control siRNA also show very few spontaneous exocytotic events in the absence of stimulation but massive exocytosis in response to depolarization. In contrast, AP-3 RNAi significantly increases baseline, constitutive exocytosis of VMAT2 and greatly reduces the response to stimulation (Fig. 5, A, C, and D; and Videos 1 and 2).

AP-3 contributes to LDCV biogenesis

How does AP-3 contribute to regulated secretion? The loss of AP-3 might have pleiotropic effects that indirectly influence the regulation of LDCV exocytosis. Alternatively, AP-3 may have a primary role in LDCV production that influences their composition and, consequently, their fusion. We therefore characterized the properties of LDCVs produced in the absence of this adaptor. Separating PC12 membranes by equilibrium sedimentation through sucrose, we find that the knockdown of AP-3 reduces the proportion of SgII migrating in fractions that would, in control cells, contain LDCVs. AP-3 RNAi also shifts SgII to lighter fractions (Fig. 6 A). In separate experiments, we took advantage of cotransfected ANF-GFP to assay more (~80) gradient fractions using a fluorescent plate reader and to achieve higher resolution. Like endogenous SgII, ANF-GFP shows a shift toward light fractions with AP-3 RNAi (Fig. 6 B). Importantly, the RNAi has no effect on migration of the synaptic vesicle protein synaptophysin (Fig. 6 A). Thus, AP-3 has a specific effect on the properties of LDCVs, suggesting that any defect in fusion results from a change in their composition and therefore their formation.

To determine whether AP-3 RNAi affects the number of LDCVs and their morphology, we used electron microscopy. The analysis shows a substantial reduction in the number and density of LDCVs in PC12 cells subjected to knockdown of AP-3 (Fig. 6 C), which is consistent with a role for AP-3 in their production. As suggested by previous work (Grabner et al., 2006), the size of LDCVs also increases significantly with a reduction in AP-3 (Fig. 6 D).

To assess a specific role for AP-3 in LDCV production, we used metabolic labeling with $^{35}SO_4^-$, which occurs specifically within the TGN (Baeuerle and Huttner, 1987), where LDCVs form. Sulfation labels both SgII and the constitutively secreted heparan sulfate proteoglycan (HSPG; Tooze and Huttner, 1990). 4 h after labeling, $^{35}SO_4^-$-HSPG essentially disappears from control PC12 cells, which is consistent with constitutive release, and this does not change with AP-3 RNAi (Fig. 7 A). In contrast, $^{35}SO_4^-$-SgII undergoes prolonged storage in control PC12 cells. However, in cells lacking AP-3, $^{35}SO_4^-$-SgII undergoes constitutive secretion. Analysis of the medium confirms the constitutive release of $^{35}SO_4^-$-HSPG that is unaffected by AP-3 RNAi and the dysregulated secretion of $^{35}SO_4^-$-SgII produced by loss of AP-3 (Fig. 7 B). AP-3 thus influences the fate of LDCVs rather than constitutive secretory vesicles, which is consistent with a specific role in formation of the RSP.

AP-3 might influence either the biogenesis of LDCVs at the TGN or the process of maturation after budding that involves the removal of proteins destined for other organelles (Morvan and Tooze, 2008). The adaptor AP-1 rather than AP-3 has been implicated in LDCV maturation (Dittie et al., 1996), but to assess a distinct role for AP-3 in budding from the TGN, we again used metabolic labeling with $^{35}SO_4^-$, allowing only 15 min of chase to enable a direct analysis of the newly formed vesicles (Tooze and Huttner, 1990). These vesicles were separated from the TGN donor compartment by velocity centrifugation through sucrose, the top fractions (1–5) were pooled, and LDCVs were further separated from constitutive secretory vesicles by equilibrium sedimentation through sucrose. In PC12 cells treated with control siRNA, the constitutively secreted $^{35}SO_4^-$-HSPG migrates in fractions 8–10, whereas LDCV protein $^{35}SO_4^-$-SgII migrates in fractions 12–13 (Fig. 7 C). In contrast, AP-3 RNAi shifts the $^{35}SO_4^-$-SgII signal toward lighter fractions partially overlapping with the $^{35}SO_4^-$-HSPG signal. The redistribution of $^{35}SO_4^-$-SgII shows that AP-3 promotes sorting into LDCVs at the level of the TGN.

The shift in LDCV proteins to lighter fractions suggests that in the absence of AP-3, LDCV cargo may sort instead to constitutive secretory vesicles. Indeed, vesicles with dense cores still bud without AP-3, and the presence of a dense core may account for their intermediate density. To reconcile the mild morphological phenotype of AP-3 RNAi with the severe functional effect on secretion, we examined the distribution of membrane proteins implicated in regulated exocytosis. Equilibrium sedimentation through sucrose shows that the v-SNAREs VAMP2 and -3 migrate over a wide range of fractions with enrichment in lighter membranes, but the distribution shows no clear change with RNAi for AP-3 (Fig. 8 A). In contrast, AP-3 RNAi redistributes the calcium sensor synaptotagmin 1 (Fernández-Chacón et al., 2001; Chapman, 2008) from heavy to light membranes (Fig. 8), a dramatic effect that presumably contributes to the gross disturbance in regulated secretion.

Discussion

An RNAi screen identifies genes required for sorting to the RSP

Using a sensitive reporter, RNAi in *Drosophila* S2 cells, and high-throughput flow cytometry, we identified a remarkably

peak (black line), expressed as a percentage of total area. *, $P < 0.01$ relative to control by two-tailed Student's *t* test ($n = 3$ transfections). (C and D) PC12 cells were transfected twice with either control or AP-3 siRNA and processed for electron microscopy 2 d after the second transfection. (C) Low magnification electron micrographs show a large reduction in the number of LDCVs (arrowheads) of cells transfected with AP-3 siRNA (right) relative to controls (left). Bar graphs indicate the number of LDCVs per cell in the section (left) and LDCV density (right). *, $P < 0.0005$; **, $P < 0.000001$ ($n = 20$ cells/condition). (D) Higher magnification electron micrographs show that AP-3 RNAi increases the size of LDCVs. Bar graphs indicate the corrected diameters (left) and areas (right) of both the entire LDCV and the electron-dense core (Parsons et al., 1995). (bottom) The LDCV area is presented as a frequency histogram. *, $P < 0.01$ ($n = 205–221$ LDCVs/condition). Bars, 200 nm.

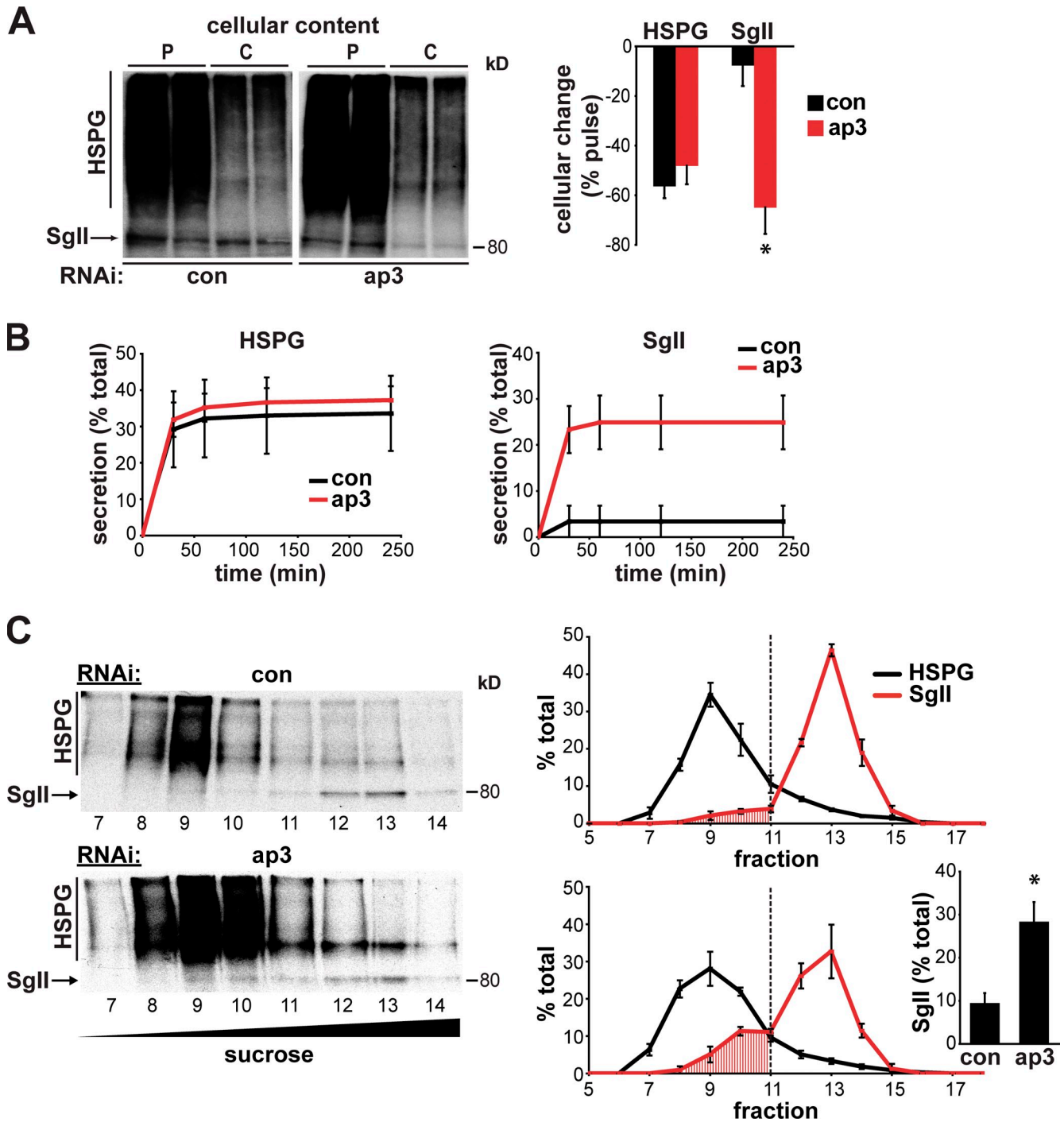

Figure 7. **AP-3 RNAi diverts SgII to constitutive secretory vesicles budding from the TGN.** (A and B) PC12 cells were transfected twice with 50 nM AP-3 or control siRNA, labeled for 5 min with 0.5–1 mCi/ml $^{35}SO_4$, and either harvested directly (pulse [p]) or incubated at 37°C for 4 h (chase [c]) in complete medium containing 1.6 mM nonradioactive Na_2SO_4. (A) Separation of duplicate cell extracts by electrophoresis followed by autoradiography shows that after 4 h, control cells store almost all of the labeled SgII. In contrast, AP-3 RNAi dramatically reduces the storage of SgII with no effect on the constitutively secreted HSPG. Error bars indicate the percent decline in cellular content of labeled protein after the chase relative to just after the pulse. *, $P < 0.02$ relative to control by two-tailed Student's *t* test ($n = 3$). (B) Aliquots of media from the times indicated confirm the constitutive secretion of HSPG unaffected by AP-3 RNAi and the constitutive release of SgII produced by AP-3 RNAi. (C) PC12 were transfected and labeled with $^{35}SO_4$ as described in A, incubated at 37°C for 15 min after the pulse, and a postnuclear supernatant separated by velocity sedimentation through a 0.3–1.2 M continuous sucrose gradient, with the TGN-derived vesicles in fractions 1–5 separated further by equilibrium sedimentation on a 0.5–2 M continuous sucrose gradient. (left) 500 µl fractions were collected from the top of the gradient, and 50 µl aliquots were separated by electrophoresis followed by fluorography. (right) Only fractions with significant amounts of radioactivity are shown, and the labeled HSPG and SgII in each fraction are expressed as a percentage of the total labeled protein on the gradient. The amount of SgII in the HSPG peak increases with AP-3 RNAi, and the bar graph indicates the area under the HSPG peak as a percentage of the area under the entire SgII curve (inset). *, $P < 0.05$ relative to control by two-tailed Student's *t* test. The data indicate means of three independent transfections, and error bars indicate SEM.

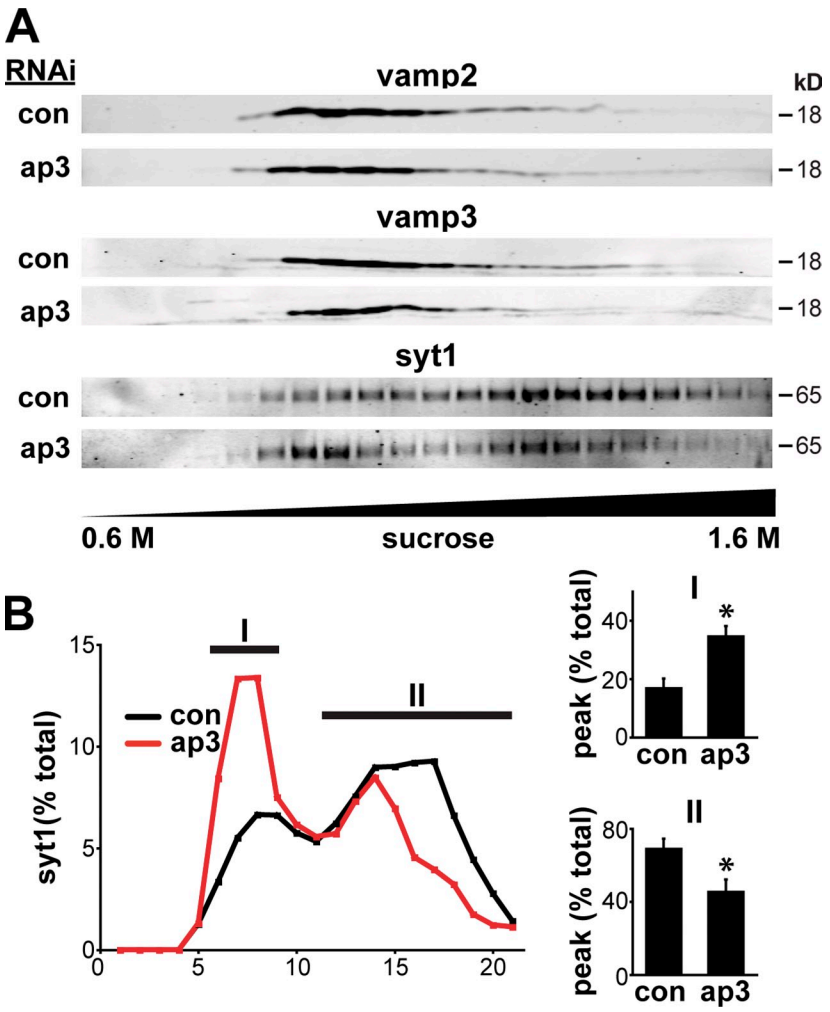

Figure 8. **AP-3 RNAi affects the membrane composition of LDCVs.** PC12 cells were transfected twice with 50 nM AP-3δ or control siRNA, and the postnuclear supernatant obtained 2–3 d after the second transfection separated by equilibrium sedimentation through 0.6–1.6 M sucrose. (A) Fractions were collected from the top of the gradient and assayed for VAMP2, VAMP3, and synaptotagmin 1 (syt1) by quantitative fluorescent immunoblotting. (B) The amounts in each fraction in light membranes (peak I) and LDCV fractions (peak II) are expressed as a percentage of total gradient immunoreactivity. AP-3 RNAi greatly reduces the LDCV peak of synaptotagmin 1 and shifts the synaptotagmin 1 immunoreactivity toward lighter fractions. *, $P < 0.05$ relative to control by two-tailed Student's *t* test ($n = 3$ transfections). Error bars indicate SEM.

small number of genes required for sorting to the RSP. Most of these have a known role in membrane trafficking, but only four are required for regulated secretion.

Classifying the genes further in terms of their functional interaction with the cytosolic dileucine-like motif in VMAT (and in particular the upstream acidic residues), we found that the knockdown of two genes (*nup93* and *pp1-13c*) increases cell surface expression of both DE/AA and wt dVMAT (class I). Although a subunit of the nuclear pore complex, nup93 exhibits structural similarity to coat proteins, and one subunit of the COPII coat indeed belongs to a subcomplex of the nuclear pore (Devos et al., 2004; Brohawn et al., 2008). Considering its localization to the nuclear envelope, nup93 may thus have a role in sorting to the RSP at the level of the endoplasmic reticulum, where sorting may begin (Martínez-Menárguez et al., 1999). Knockdown of the catalytic subunit in PP1 also impairs regulated secretion, and several kinases have been implicated in sorting at the TGN. In addition to lipid kinases, which synthesize the phosphatidylinositol-4-phosphate required for recruitment of multiple proteins to the Golgi complex (De Matteis and Luini, 2008), protein kinase D contributes to constitutive secretion (Liljedahl et al., 2001). PP1 may promote sorting to the RSP by antagonizing the function of these kinases, thereby regulating the production of LDCVs and constitutive secretory vesicles.

Among the dsRNA whose effects are occluded by the DE/AA mutation (class III genes), we identified a carboxypeptidase that influences regulated exocytosis. Interestingly, previous work has suggested that the membrane-associated protease carboxypeptidase E promotes sorting to the RSP of multiple peptides, including proopiomelanocortin and insulin (Cool et al., 1997; Cawley et al., 2004). However, the carboxypeptidase identified in this screen is required for the trafficking of VMAT, a polytopic membrane protein that does not undergo proteolytic processing, and for the regulated secretion of ANF. In addition, the gene identified in this study shows stronger similarity to the carboxypeptidase B than the E family.

AP-3 is required for sorting to the regulated pathway

The screen also identified multiple subunits of the adaptor protein AP-3. The knockdown of these subunits produces some of the strongest effects on surface expression of dVMAT, and the most profound on ANF, with increased constitutive and reduced regulated secretion. Furthermore, we find that AP-3 RNAi increases VMAT2 surface expression in PC12 cells and markedly impairs the regulated secretion of SgII from this mammalian cell line.

Like other class III genes, the DE/AA mutation occludes the effect of AP-3 RNAi, suggesting that they act in the same

pathway. Consistent with this, a previous study has suggested that the interaction of a dileucine motif with AP-3 requires acidic residues 4 and 5 upstream (Janvier et al., 2003) at the same positions found in dVMAT, mammalian VMAT2, and phogrin. Moreover, a recent study on the closely related adaptor AP-2 suggests a structural basis for the more stringent requirement of AP-3 for upstream acidic residues (Kelly et al., 2008). Although it can be difficult to assess the relevance of adaptor–cargo interactions identified in vitro, the study now provides functional evidence that AP-3 interacts directly with the extended dileucine motif in VMAT2 to mediate its sorting into the RSP.

The results show that the loss of AP-3 disrupts the regulated exocytosis of LDCVs. AP-3 RNAi almost eliminates the regulated release of SgII from PC12 cells, with only a minimal effect on the amount secreted constitutively. However, because AP-3 knockdown reduces the cellular content of SgII, it increases the proportion that undergoes constitutive release. Importantly, the loss of AP-3 greatly reduces the storage of granin proteins in *mocha* mice and PC12 cells, establishing the physiological relevance of the findings in vitro and excluding potential off-target effects of the RNAi. In addition, the analysis of VMAT2 exocytosis by direct optical imaging demonstrates both an increase in constitutive release and a dramatic reduction in regulated release produced by the loss of AP-3.

AP-3 has previously been suggested to influence the morphology of LDCVs. The *mocha* mutation increases the size of chromaffin granules by direct electrochemical measurement of quantal monoamine release and electron microscopy (Grabner et al., 2006). We also observe enlarged LDCVs after AP-3 knockdown in PC12 cells. However, Grabner et al. (2006) examined release only after the direct application of calcium to permeabilized cells and did not address the regulation of release. Thus, the results presented in this study provide the first evidence that AP-3 is required for regulated secretion.

AP-3 influences LDCV formation

To understand how the loss of AP-3 disrupts regulated exocytosis, we examined the effect on LDCVs. In addition to the increased diameter, we observe a major reduction (~50%) in the number of LDCVs. Soluble LDCV cargo (endogenous SgII and transfected ANF-GFP) also shifts toward lighter fractions by equilibrium sedimentation. These effects strongly suggest that AP-3 contributes to LDCV formation or maturation rather than simply to their regulated exocytosis.

We took advantage of labeling with $^{35}SO_4^-$ to determine how AP-3 influences the fate of secretory vesicles formed at the TGN. In contrast to control cells that release negligible amounts of SgII even after 4 h of chase, AP-3 RNAi results in the release of SgII within 30 min after budding from the TGN, with no effect on the constitutively released HSPG. Because LDCV maturation continues long after budding from the TGN, the rapid release of SgII suggests a role for AP-3 that precedes maturation, such as sorting within the TGN. Consistent with an earlier locus for AP-3 action, LDCV maturation is apparently not required for the regulation of exocytosis (Tooze et al., 1991).

To address a role for AP-3 in sorting at the TGN, we examined the formation of secretory vesicles 15 min after labeling with $^{35}SO_4^-$. At this time, vesicles containing $^{35}SO_4^-$-SgII and -HSPG have budded from the TGN, and equilibrium sedimentation can be used to separate light constitutive secretory vesicles (containing HSPG) from heavier immature LDCVs (containing SgII). Using this assay, we find that the loss of AP-3 redistributes SgII into lighter fractions. Although the missorting is again not complete, it is similar to that observed at steady state for SgII and for EE/AA rat VMAT2 (Krantz et al., 2000). These results indicate that AP-3 has a role in sorting to LDCVs at the level of the TGN.

AP-3 has generally been considered to function within the endocytic rather than biosynthetic pathway. AP-3 mediates sorting to lysosomes and LROs such as melanosomes and secretory lysosomes (Newell-Litwa et al., 2007; Dell'Angelica, 2009), and these membranes, in contrast to LDCVs, form within the endocytic pathway. Loss of AP-3 also affects the behavior of lytic granules, the LROs of cytotoxic T cells, but does not influence the sorting of soluble cargo into lytic granules, and this has again been attributed to a defect in the endocytic pathway (Clark et al., 2003). Consistent with this role, AP-3 localizes primarily to endosomes (Peden et al., 2004). However, lower levels also localize to other sites, including the Golgi complex (Dell'Angelica et al., 1997; Peden et al., 2004). In addition, AP-3 contains neural and ubiquitous subunits, and we do not know whether they have the same subcellular distribution. It is also possible that AP-3 on endosomes promotes sorting to the RSP by recycling to the TGN components required for LDCV formation, but AP-3 promotes recycling to lysosomes and LROs, not the Golgi complex (Dell'Angelica, 2009). Although unanticipated from previous work, the requirement for AP-3 in sorting to the RSP now argues for a functional role in the biosynthetic pathway, at the TGN.

Supporting a role in the biosynthetic pathway, AP-3 functions at the TGN in yeast (Cowles et al., 1997; Stepp et al., 1997). In contrast to the main lysosomal targeting pathway that delivers hydrolases such as carboxypeptidase Y to the vacuole through an endosomal intermediate, AP-3 contributes to an alternative pathway that targets alkaline phosphatase directly to the vacuole. However, this pathway has been considered specific to yeast. The evidence of a role for AP-3 in sorting to the RSP now suggests that a component of the alternative lysosome-targeting pathway participates directly in the formation of regulated secretory vesicles from the TGN of metazoans. Because the alternative lysosome-targeting pathway lacks an endosomal intermediate, it may have been particularly well suited to minimize the loss of soluble cargo and acquire the capacity for regulated release of proteins that mediate extracellular signaling.

Despite the effects of AP-3 loss on LDCV number, morphology, and density, vesicles with a dense core still form both in PC12 cells after RNAi and in *mocha* mice. What then accounts for the disproportionately severe functional effect on regulated exocytosis? The budding assay suggests that proteins normally segregated to the RSP intermix with those destined for constitutive secretion, and this may account for the intermediate density and increased size of vesicles with a dense core. Supporting this possibility, we find that the loss of AP-3 redistributes synaptotagmin 1 to fractions even lighter than those containing

soluble LDCV cargo. As a major calcium sensor for regulated exocytosis of LDCVs (Voets et al., 2001; Schonn et al., 2008), the change in synaptotagmin distribution presumably contributes to the loss of regulated release. In addition, previous work on the trafficking of synaptotagmin 1 has identified a conserved C-terminal dileucine motif with upstream acidic residues (*EE*VDA**ML**) that may account for the dependence on AP-3 (Blagoveshchenskaya et al., 1999; Jarousse and Kelly, 2001). However, the effect of AP-3 deficiency seems more profound than that produced by loss of synaptotagmin 1 (Voets et al., 2001; Schonn et al., 2008), strongly suggesting that AP-3 also affects the distribution of other proteins that influence the mode of exocytosis.

Materials and methods

Molecular biology

EGFP or mCherry were fused to the N terminus of HA-dVMAT (provided by D. Krantz, University of California, Los Angeles, Los Angeles, CA) to produce GFP-/HA-dVMAT and mCherry-/HA-dVMAT, respectively. The DE/AA mutation was introduced by overlap extension PCR. ANF-GFP was provided by E. Levitan (University of Pittsburgh, Pittsburgh, PA), and ss-GFP was constructed by amplifying the ss of ANF and fusing it directly to GFP. For expression in *Drosophila* S2 cells, all cDNAs were subcloned into pAc5.1 (Invitrogen). For expression in rat PC12 cells, all cDNAs were subcloned into the chicken actin-based vector pCAGGS.

Cell culture

Drosophila S2 cells were maintained in Schneider medium (Invitrogen) supplemented with 10% heat-inactivated fetal bovine serum at 27°C in a humidified incubator. Transfection of S2 cells was performed using either Nucleofection (Lonza) for transient expression or Fugene HD reagent (Roche) for stable expression, both according to the manufacturer's instructions. For stable expression, S2 cells were cotransfected with GFP-/HA-dVMAT and pCoHygro (Invitrogen) in a 10:1 molar ratio and selected in 300 µg/ml hygromycin for 4 wk. PC12 cells were maintained in DME-H21 medium supplemented with 10% horse serum and 5% calf serum at 37°C. Transfection of PC12 cells was performed using Lipofectamine 2000 (Invitrogen) according to the manufacturer's instructions.

Antibodies and immunofluorescence

The HA.11 mouse monoclonal antibody was obtained from Covance, the M2-Flag mouse monoclonal antibody from Sigma-Aldrich, the SgII rabbit antibody from Meridian Life Science, the chromogranin A goat antibody from Santa Cruz Biotechnology, Inc., the σ3A mouse monoclonal antibody from BD, the VAMP2, -3, and synaptotagmin 1 antibodies from Synaptic Systems GmbH, the actin mouse monoclonal antibody from Millipore, the Zenon Alexa Fluor 647 labeling kit from Invitrogen, and the synaptophysin (p38) monoclonal antibody from Sigma-Aldrich.

Screen and analysis

S2 cells transfected with GFP-dVMAT-HA were treated in 96-well plates with dsRNA prepared from the University of California San Francisco (San Francisco, CA) DmRNAi library version 1 (7,216 genes; Goshima et al., 2007). After growth for 72 h, the cells were again treated with the same dsRNA, incubated for an additional 72 h, and surface HA expression was determined by adding external HA.11 antibody bound to Zenon Alexa Fluor 647 (1:1,000) for 2 h in standard medium, removing the unbound antibody with two washes, and subjecting the cells to high-throughput flow cytometry (lsrII; BD) for both GFP and Alexa Fluor 647 fluorescence. The ratio of Alexa Fluor 647 to GFP fluorescence was calculated for individual cells, and the mean ratio was calculated from all cells in the well.

Assuming that treatment with most dsRNA does not affect surface dVMAT expression, the mean Alexa Fluor 647/GFP fluorescence ratio from all wells of a plate should resemble the ratio from cells without dsRNA and, thus, serve as a within-plate negative control. Z scores were determined by subtracting the overall mean Alexa Fluor 647/GFP ratio (derived from the entire plate) from the ratios for individual wells, normalizing to the standard deviation determined from the mean ratios of all wells in the plate. This analysis limits statistical artifacts caused by interplate variability and has been widely used for high-throughput, cell-based screens (Malo et al., 2006), with a script written for the statistical software "R" to automate the analysis. To minimize false positives, a stringent z score > 3.0 ($P < 0.0014$) was used to identify dsRNA sequences positive in the screen. The screen was also performed twice, once using transiently transfected S2 cells, and once with stable transformants. The positives from both screens were combined, and those with few remaining cells or altered GFP expression were removed from further consideration, leaving 18 sequences (0.25% of the original library) available for further study.

To exclude off-target effects, we retested the 18 positives with non-overlapping dsRNA sequences from the same gene. In each experiment, the cumulative frequency distribution of fluorescence ratios from individual cells was plotted, compared with control RNAi, and statistical significance was analyzed by Kolmogorov-Smirnov. We applied the stringent Bonferroni correction for 19 samples (18 positives + control) and considered as positive a P value < 0.0025 in at least two independent experiments. A typical dataset consisted of 50–500 cells per dsRNA treatment in the screen and 1,000–5,000 cells in the retest. Of 18 positives from the original screen, 16 showed a consistent increase in dVMAT cell surface expression on retest and were thus considered true positives.

Secretion assays

S2 cells transfected with ANF-GFP were washed with PBS, resuspended in Tyrode's medium (119 mM NaCl, 2.5 mM KCl, 2 mM $CaCl_2$, 2 mM $MgCl_2$, 30 mM glucose, and 25 mM Hepes, pH 7.4), split equally into two tubes, incubated in the presence or absence of 100 µg/ml LPS (Sigma-Aldrich) for 1 h at 27°C, sedimented, and the fluorescence from 200 µl aliquots of the supernatant was measured in triplicate using a plate reader (Tecan), with stimulated secretion expressed as a percentage of the respective unstimulated condition.

siRNAs to rat AP-3δ1 (antisense, 5′-UUCUUGGUCAUGAUCCA-UGTG-3′; sense control, 5′-CAUGGAUCAUGACCAAGAATT-3′) were transfected twice (at 50 nM) 2 d apart, and the PC12 cells were washed 2–3 d later and incubated in Tyrode's buffer containing 2.5 mM K^+ (basal) or 90 mM K^+ (stimulated) for 30 min at 37°C. The supernatant was collected, cell lysates were prepared as previously described (Li et al., 2005), and the samples were analyzed by quantitative fluorescent immunoblotting.

Adrenal gland granin content

Mocha mice (Jackson ImmunoResearch Laboratories, Inc.) were backcrossed to C57BL/6 to remove *grizzled* and *Pde6b*^{rd1} alleles, and the adrenal glands were homogenized in 150 mM NaCl, 50 mM Tris-HCl, pH 8.0, 1% NP-40, 0.5% sodium deoxycholate, and protease inhibitors including 1 mM EGTA and 1 mM PMSF. After sedimentation at 14,000 *g* to remove nuclei and cell debris, 20 µg protein was separated by electrophoresis through polyacrylamide, transferred to nitrocellulose, and the membranes were immunoblotted for SgII and CgA, with actin as loading control and the appropriate secondary antibodies conjugated to IRDye800 (Rockland Immunochemicals, Inc.). The immunoreactivity was quantified by imaging with an Odyssey system (LI-COR Biosciences) and ImageJ (National Institutes of Health), and results were normalized to actin.

TIRF microscopy

For TIRF microscopy, PC12 cells plated onto glass chambers coated with poly-L-lysine were transfected with 50 nM siRNAs to rat AP-3δ, and 2 d later, cotransfected with siRNAs and VMAT2-pHluorin. After an additional 3 d, images were collected for 100 ms at 2 Hz and room temperature using a TIRF inverted microscope (TE2000E; Nikon) with a Plan Apo NA 1.49 100× oil objective and an electron-multiplying charge-coupled device camera (QuantEM; Photometrics). To reveal surface and total VMAT2 fluorescence, cells were incubated sequentially with Tyrode's solution containing 25 mM MES, pH 6.5, and then 50 mM NH_4Cl, pH 7.4. To examine basal and regulated release, cells were incubated in Tyrode's solution containing 2.5 mM or 90 mM K^+, respectively, for 1 min each. Videos 1 and 2 were acquired in Advanced Research (NIS-Elements), exported as AVI files, and image sequences were analyzed using ImageJ software.

Density gradient fractionation

Equilibrium sedimentation through sucrose was performed as previously described (Waites et al., 2001). In brief, a postnuclear supernatant was prepared from PC12 cells by homogenization with a ball-bearing device (8-µm clearance), loaded onto a 0.6–1.6 M continuous sucrose gradient, and sedimented at 30,000 rpm in a rotor (SW41; Beckman Coulter) for 14–16 h at 4°C. Fractions (~200 µl each) were collected from the top directly into a 96-well plate (Costar), and ANF-GFP fluorescence was read

using a plate reader (Tecan). For SgII and p38, pools of four fractions were analyzed by quantitative fluorescent immunoblotting.

Electron microscopy

PC12 cells were plated onto aclar film discs (Pella) coated with poly-L-lysine, transfected twice with 50 nM siRNA, washed with calcium-/magnesium-free PBS 2 d after the second transfection and fixed with 2.5% glutaraldehyde in calcium-/magnesium-free PBS. The discs were washed three times with 0.1 M sodium cacodylate buffer, pH 7.2, and postfixed for 30 min on ice with 1% osmium tetroxide in cacodylate buffer containing 1.6% potassium ferricyanide. The discs were then washed three times with cacodylate buffer, three times with water, incubated with 0.5% uranyl acetate for 30 min (in the dark), and washed again with water. The samples were dehydrated in a graded series of ethanols while progressively lowering the temperature from 4°C to −40°C then embedded in epon resin. After peeling off the aclar, 60-nm sections were cut and viewed in an electron microscope (FEI Tecnai 12; Phillips) at 120 kV, capturing images with a digital camera at 6,800 magnification, and analyzing them with ImageJ. Morphologically identifiable LDCVs were counted for each cell sectioned, and the cytoplasmic area was determined by subtracting the area of the nucleus from the whole cell. Density was calculated as the number of LDCVs per cell section divided by the cytoplasmic area. Corrected LDCV and core diameters were determined as previously described (Parsons et al., 1995).

Budding assay

Vesicle budding from the TGN was examined as previously described (Tooze and Huttner, 1990). In brief, PC12 cells were depleted of endogenous SO_4 for 25 min, labeled for 5 min with 0.5–1 mCi/ml $^{35}SO_4$, and chased for 15 min in complete medium containing 1.6 mM nonradioactive Na_2SO_4. The cells were homogenized with a ball-bearing device, debris sedimented, the resulting postnuclear supernatant was loaded onto a 0.3–1.2 M continuous sucrose gradient, and the newly formed vesicle was separated from the TGN by velocity centrifugation for 19 min at 4°C in an SW41 rotor at 25,000 rpm. 1 ml fractions were collected from the top of the gradient, and pooled fractions 1–5 were loaded onto a 0.5–2 M continuous sucrose gradient sedimented to equilibrium (SW41) at 25,000 rpm and 4°C for 16 h. 500 µl fractions were collected from the top of the gradient, and 50 µl aliquots were separated by electrophoresis through polyacrylamide followed by fluorography and quantitation of the resulting images by densitometry.

Online supplemental material

Fig. S1 shows the colocalization in *Drosophila* S2 cells of dVMAT-cherry with ANF-GFP but not ss-GFP, which is consistent with the sorting of dVMAT to the RSP. Video 1 shows the stimulation of VMAT2-pHluorin exocytosis by TIRF microscopy in PC12 cells transfected with control siRNA and depolarized with 90 mM K^+. Video 2 shows the high rate of constitutive VMAT2-pHluorin exocytosis in PC12 cells transfected with AP-3δ siRNA and the minimal increase evoked by depolarization with high K^+. Online supplemental material is available at http://www.jcb.org/cgi/content/full/jcb.201006131/DC1.

We thank the laboratories of E. Brown, G. Davis, and R. Vale for help initiating these experiments, J.S. Weissman and J. DeRisi for assistance with the high-throughput cell sorter, Kurt Thorn and the University of California San Francisco Nikon Imaging Center for guidance with the TIRF microscopy.

This work was supported by a fellowship from the Swiss National Science Foundation (to C.S. Asensio), a predoctoral fellowship from the National Institute of Mental Health (to D.W. Sirkis), and a grant from the National Institute on Drug Abuse (P01 to R.H. Edwards).

Submitted: 22 June 2010
Accepted: 9 November 2010

References

Arvan, P., and D. Castle. 1998. Sorting and storage during secretory granule biogenesis: looking backward and looking forward. *Biochem. J.* 332:593–610.

Baeuerle, P.A., and W.B. Huttner. 1987. Tyrosine sulfation is a trans-Golgi-specific protein modification. *J. Cell Biol.* 105:2655–2664. doi:10.1083/jcb.105.6.2655

Bard, F., L. Casano, A. Mallabiabarrena, E. Wallace, K. Saito, H. Kitayama, G. Guizzunti, Y. Hu, F. Wendler, R. Dasgupta, et al. 2006. Functional genomics reveals genes involved in protein secretion and Golgi organization. *Nature.* 439:604–607. doi:10.1038/nature04377

Berwin, B., E. Floor, and T.F. Martin. 1998. CAPS (mammalian UNC-31) protein localizes to membranes involved in dense-core vesicle exocytosis. *Neuron.* 21:137–145. doi:10.1016/S0896-6273(00)80521-8

Blagoveshchenskaya, A.D., E.W. Hewitt, and D.F. Cutler. 1999. Di-leucine signals mediate targeting of tyrosinase and synaptotagmin to synaptic-like microvesicles within PC12 cells. *Mol. Biol. Cell.* 10:3979–3990.

Blagoveshchenskaya, A.D., M.J. Hannah, S. Allen, and D.F. Cutler. 2002. Selective and signal-dependent recruitment of membrane proteins to secretory granules formed by heterologously expressed von Willebrand factor. *Mol. Biol. Cell.* 13:1582–1593. doi:10.1091/mbc.01-09-0462

Brohawn, S.G., N.C. Leksa, E.D. Spear, K.R. Rajashankar, and T.U. Schwartz. 2008. Structural evidence for common ancestry of the nuclear pore complex and vesicle coats. *Science.* 322:1369–1373. doi:10.1126/science.1165886

Burman, J.L., L. Bourbonniere, J. Philie, T. Stroh, S.Y. Dejgaard, J.F. Presley, and P.S. McPherson. 2008. Scyl1, mutated in a recessive form of spinocerebellar neurodegeneration, regulates COPI-mediated retrograde traffic. *J. Biol. Chem.* 283:22774–22786. doi:10.1074/jbc.M801869200

Cawley, N.X., J. Zhou, J.M. Hill, D. Abebe, S. Romboz, T. Yanik, R.M. Rodriguiz, W.C. Wetsel, and Y.P. Loh. 2004. The carboxypeptidase E knockout mouse exhibits endocrinological and behavioral deficits. *Endocrinology.* 145:5807–5819. doi:10.1210/en.2004-0847

Chapman, E.R. 2008. How does synaptotagmin trigger neurotransmitter release? *Annu. Rev. Biochem.* 77:615–641. doi:10.1146/annurev.biochem.77.062005.101135

Chavez, R.A., S.G. Miller, and H.P. Moore. 1996. A biosynthetic regulated secretory pathway in constitutive secretory cells. *J. Cell Biol.* 133:1177–1191. doi:10.1083/jcb.133.6.1177

Chen, Z.Y., A. Ieraci, H. Teng, H. Dall, C.X. Meng, D.G. Herrera, A. Nykjaer, B.L. Hempstead, and F.S. Lee. 2005. Sortilin controls intracellular sorting of brain-derived neurotrophic factor to the regulated secretory pathway. *J. Neurosci.* 25:6156–6166. doi:10.1523/JNEUROSCI.1017-05.2005

Clark, R.H., J.C. Stinchcombe, A. Day, E. Blott, S. Booth, G. Bossi, T. Hamblin, E.G. Davies, and G.M. Griffiths. 2003. Adaptor protein 3-dependent microtubule-mediated movement of lytic granules to the immunological synapse. *Nat. Immunol.* 4:1111–1120. doi:10.1038/ni1000

Cool, D.R., E. Normant, F. Shen, H.C. Chen, L. Pannell, Y. Zhang, and Y.P. Loh. 1997. Carboxypeptidase E is a regulated secretory pathway sorting receptor: genetic obliteration leads to endocrine disorders in Cpe(fat) mice. *Cell.* 88:73–83. doi:10.1016/S0092-8674(00)81860-7

Cowles, C.R., G. Odorizzi, G.S. Payne, and S.D. Emr. 1997. The AP-3 adaptor complex is essential for cargo-selective transport to the yeast vacuole. *Cell.* 91:109–118. doi:10.1016/S0092-8674(01)80013-1

De Matteis, M.A., and A. Luini. 2008. Exiting the Golgi complex. *Nat. Rev. Mol. Cell Biol.* 9:273–284. doi:10.1038/nrm2378

Dell'Angelica, E.C. 2009. AP-3-dependent trafficking and disease: the first decade. *Curr. Opin. Cell Biol.* 21:552–559. doi:10.1016/j.ceb.2009.04.014

Dell'Angelica, E.C., H. Ohno, C.E. Ooi, E. Rabinovich, K.W. Roche, and J.S. Bonifacino. 1997. AP-3: an adaptor-like protein complex with ubiquitous expression. *EMBO J.* 16:917–928. doi:10.1093/emboj/16.5.917

Devos, D., S. Dokudovskaya, F. Alber, R. Williams, B.T. Chait, A. Sali, and M.P. Rout. 2004. Components of coated vesicles and nuclear pore complexes share a common molecular architecture. *PLoS Biol.* 2:e380. doi:10.1371/journal.pbio.0020380

Dittie, A.S., N. Hajibagheri, and S.A. Tooze. 1996. The AP-1 adaptor complex binds to immature secretory granules from PC12 cells, and is regulated by ADP-ribosylation factor. *J. Cell Biol.* 132:523–536. doi:10.1083/jcb.132.4.523

Eaton, B.A., M. Haugwitz, D. Lau, and H.P. Moore. 2000. Biogenesis of regulated exocytotic carriers in neuroendocrine cells. *J. Neurosci.* 20:7334–7344.

Elhamdani, A., T.F. Martin, J.A. Kowalchyk, and C.R. Artalejo. 1999. Ca(2+)-dependent activator protein for secretion is critical for the fusion of dense-core vesicles with the membrane in calf adrenal chromaffin cells. *J. Neurosci.* 19:7375–7383.

Erickson, J.D., L.E. Eiden, M.K. Schafer, and E. Weihe. 1995. Reserpine- and tetrabenazine-sensitive transport of (3)H-histamine by the neuronal isoform of the vesicular monoamine transporter. *J. Mol. Neurosci.* 6:277–287. doi:10.1007/BF02736786

Fernández-Chacón, R., A. Königstorfer, S.H. Gerber, J. García, M.F. Matos, C.F. Stevens, N. Brose, J. Rizo, C. Rosenmund, and T.C. Südhof. 2001. Synaptotagmin I functions as a calcium regulator of release probability. *Nature.* 410:41–49. doi:10.1038/35065004

Foley, E., and P.H. O'Farrell. 2004. Functional dissection of an innate immune response by a genome-wide RNAi screen. *PLoS Biol.* 2:E203. doi:10.1371/journal.pbio.0020203

Goshima, G., R. Wollman, S.S. Goodwin, N. Zhang, J.M. Scholey, R.D. Vale, and N. Stuurman. 2007. Genes required for mitotic spindle assembly

in *Drosophila* S2 cells. *Science.* 316:417–421. doi:10.1126/science.1141314

Grabner, C.P., S.D. Price, A. Lysakowski, A.L. Cahill, and A.P. Fox. 2006. Regulation of large dense-core vesicle volume and neurotransmitter content mediated by adaptor protein 3. *Proc. Natl. Acad. Sci. USA.* 103:10035–10040. doi:10.1073/pnas.0509844103

Greer, C.L., A. Grygoruk, D.E. Patton, B. Ley, R. Romero-Calderon, H.Y. Chang, R. Houshyar, R.J. Bainton, A. Diantonio, and D.E. Krantz. 2005. A splice variant of the *Drosophila* vesicular monoamine transporter contains a conserved trafficking domain and functions in the storage of dopamine, serotonin, and octopamine. *J. Neurobiol.* 64:239–258. doi:10.1002/neu.20146

Guo, Y., T.C. Walther, M. Rao, N. Stuurman, G. Goshima, K. Terayama, J.S. Wong, R.D. Vale, P. Walter, and R.V. Farese. 2008. Functional genomic screen reveals genes involved in lipid-droplet formation and utilization. *Nature.* 453:657–661. doi:10.1038/nature06928

Harrison-Lavoie, K.J., G. Michaux, L. Hewlett, J. Kaur, M.J. Hannah, W.W. Lui-Roberts, K.E. Norman, and D.F. Cutler. 2006. P-selectin and CD63 use different mechanisms for delivery to Weibel-Palade bodies. *Traffic.* 7:647–662. doi:10.1111/j.1600-0854.2006.00415.x

Janvier, K., Y. Kato, M. Boehm, J.R. Rose, J.A. Martina, B.Y. Kim, S. Venkatesan, and J.S. Bonifacino. 2003. Recognition of dileucine-based sorting signals from HIV-1 Nef and LIMP-II by the AP-1 γ–σ1 and AP-3 δ–σ3 hemicomplexes. *J. Cell Biol.* 163:1281–1290. doi:10.1083/jcb.200307157

Jarousse, N., and R.B. Kelly. 2001. The AP2 binding site of synaptotagmin 1 is not an internalization signal but a regulator of endocytosis. *J. Cell Biol.* 154:857–866. doi:10.1083/jcb.200103040

Kantheti, P., X. Qiao, M.E. Diaz, A.A. Peden, G.E. Meyer, S.L. Carskadon, D. Kapfhamer, D. Sufalko, M.S. Robinson, J.L. Noebels, and M. Burmeister. 1998. Mutation in AP-3 delta in the mocha mouse links endosomal transport to storage deficiency in platelets, melanosomes, and synaptic vesicles. *Neuron.* 21:111–122. doi:10.1016/S0896-6273(00)80519-X

Kelly, B.T., A.J. McCoy, K. Spate, S.E. Miller, P.R. Evans, S. Honing, and D.J. Owen. 2008. A structural explanation for the binding of endocytic dileucine motifs by the AP2 complex. *Nature.* 456:976–979. doi:10.1038/nature07422

Kim, T., J.H. Tao-Cheng, L.E. Eiden, and Y.P. Loh. 2001. Chromogranin A, an "on/off" switch controlling dense-core secretory granule biogenesis. *Cell.* 106:499–509. doi:10.1016/S0092-8674(01)00459-7

Krantz, D.E., D. Peter, Y. Liu, and R.H. Edwards. 1997. Phosphorylation of a vesicular monoamine transporter by casein kinase II. *J. Biol. Chem.* 272:6752–6759. doi:10.1074/jbc.272.10.6752

Krantz, D.E., C. Waites, V. Oorschot, Y. Liu, R.I. Wilson, P.K. Tan, J. Klumperman, and R.H. Edwards. 2000. A phosphorylation site regulates sorting of the vesicular acetylcholine transporter to dense core vesicles. *J. Cell Biol.* 149:379–395. doi:10.1083/jcb.149.2.379

Lewis, M.J., J.C. Rayner, and H.R. Pelham. 1997. A novel SNARE complex implicated in vesicle fusion with the endoplasmic reticulum. *EMBO J.* 16:3017–3024. doi:10.1093/emboj/16.11.3017

Li, H., C.L. Waites, R.G. Staal, Y. Dobryy, J. Park, D.L. Sulzer, and R.H. Edwards. 2005. Sorting of vesicular monoamine transporter 2 to the regulated secretory pathway confers the somatodendritic exocytosis of monoamines. *Neuron.* 48:619–633. doi:10.1016/j.neuron.2005.09.033

Liljedahl, M., Y. Maeda, A. Colanzi, I. Ayala, J. Van Lint, and V. Malhotra. 2001. Protein kinase D regulates the fission of cell surface destined transport carriers from the trans-Golgi network. *Cell.* 104:409–420. doi:10.1016/S0092-8674(01)00228-8

Liu, Y., E.S. Schweitzer, M.J. Nirenberg, V.M. Pickel, C.J. Evans, and R.H. Edwards. 1994. Preferential localization of a vesicular monoamine transporter to dense core vesicles in PC12 cells. *J. Cell Biol.* 127:1419–1433. doi:10.1083/jcb.127.5.1419

Malo, N., J.A. Hanley, S. Cerquozzi, J. Pelletier, and R. Nadon. 2006. Statistical practice in high-throughput screening data analysis. *Nat. Biotechnol.* 24:167–175. doi:10.1038/nbt1186

Martin, T.F., and J.H. Walent. 1989. A new method for cell permeabilization reveals a cytosolic protein requirement for Ca2+ -activated secretion in GH3 pituitary cells. *J. Biol. Chem.* 264:10299–10308.

Martínez-Menárguez, J.A., H.J. Geuze, J.W. Slot, and J. Klumperman. 1999. Vesicular tubular clusters between the ER and Golgi mediate concentration of soluble secretory proteins by exclusion from COPI-coated vesicles. *Cell.* 98:81–90. doi:10.1016/S0092-8674(00)80608-X

Miesenböck, G., D.A. De Angelis, and J.E. Rothman. 1998. Visualizing secretion and synaptic transmission with pH-sensitive green fluorescent proteins. *Nature.* 394:192–195. doi:10.1038/28190

Morvan, J., and S.A. Tooze. 2008. Discovery and progress in our understanding of the regulated secretory pathway in neuroendocrine cells. *Histochem. Cell Biol.* 129:243–252. doi:10.1007/s00418-008-0377-z

Newell-Litwa, K., E. Seong, M. Burmeister, and V. Faundez. 2007. Neuronal and non-neuronal functions of the AP-3 sorting machinery. *J. Cell Sci.* 120:531–541. doi:10.1242/jcs.03365

Onoa, B., H. Li, J.A. Gagnon-Bartsch, L.A. Elias, and R.H. Edwards. 2010. Vesicular monoamine and glutamate transporters select distinct synaptic vesicle recycling pathways. *J. Neurosci.* 30:7917–7927. doi:10.1523/JNEUROSCI.5298-09.2010

Orci, L., M. Ravazzola, M. Amherdt, A. Perrelet, S.K. Powell, D.L. Quinn, and H.P. Moore. 1987. The trans-most cisternae of the Golgi complex: a compartment for sorting of secretory and plasma membrane proteins. *Cell.* 51:1039–1051. doi:10.1016/0092-8674(87)90590-3

Parsons, T.D., J.R. Coorssen, H. Horstmann, and W. Almers. 1995. Docked granules, the exocytic burst, and the need for ATP hydrolysis in endocrine cells. *Neuron.* 15:1085–1096. doi:10.1016/0896-6273(95)90097-7

Peden, A.A., V. Oorschot, B.A. Hesser, C.D. Austin, R.H. Scheller, and J. Klumperman. 2004. Localization of the AP-3 adaptor complex defines a novel endosomal exit site for lysosomal membrane proteins. *J. Cell Biol.* 164:1065–1076. doi:10.1083/jcb.200311064

Sankaranarayanan, S., D. De Angelis, J.E. Rothman, and T.A. Ryan. 2000. The use of pHluorins for optical measurements of presynaptic activity. *Biophys. J.* 79:2199–2208. doi:10.1016/S0006-3495(00)76468-X

Schonn, J.S., A. Maximov, Y. Lao, T.C. Südhof, and J.B. Sørensen. 2008. Synaptotagmin-1 and -7 are functionally overlapping Ca2+ sensors for exocytosis in adrenal chromaffin cells. *Proc. Natl. Acad. Sci. USA.* 105:3998–4003. doi:10.1073/pnas.0712373105

Shakiryanova, D., A. Tully, R.S. Hewes, D.L. Deitcher, and E.S. Levitan. 2005. Activity-dependent liberation of synaptic neuropeptide vesicles. *Nat. Neurosci.* 8:173–178. doi:10.1038/nn1377

Speese, S., M. Petrie, K. Schuske, M. Ailion, K. Ann, K. Iwasaki, E.M. Jorgensen, and T.F. Martin. 2007. UNC-31 (CAPS) is required for dense-core vesicle but not synaptic vesicle exocytosis in *Caenorhabditis elegans*. *J. Neurosci.* 27:6150–6162. doi:10.1523/JNEUROSCI.1466-07.2007

Stepp, J.D., K. Huang, and S.K. Lemmon. 1997. The yeast adaptor protein complex, AP-3, is essential for the efficient delivery of alkaline phosphatase by the alternate pathway to the vacuole. *J. Cell Biol.* 139:1761–1774. doi:10.1083/jcb.139.7.1761

Tiede, S., S. Storch, T. Lübke, B. Henrissat, R. Bargal, A. Raas-Rothschild, and T. Braulke. 2005. Mucolipidosis II is caused by mutations in GNPTA encoding the alpha/beta GlcNAc-1-phosphotransferase. *Nat. Med.* 11:1109–1112. doi:10.1038/nm1305

Tooze, S.A., and W.B. Huttner. 1990. Cell-free protein sorting to the regulated and constitutive secretory pathways. *Cell.* 60:837–847. doi:10.1016/0092-8674(90)90097-X

Tooze, S.A., T. Flatmark, J. Tooze, and W.B. Huttner. 1991. Characterization of the immature secretory granule, an intermediate in granule biogenesis. *J. Cell Biol.* 115:1491–1503. doi:10.1083/jcb.115.6.1491

Torii, S., N. Saito, A. Kawano, S. Zhao, T. Izumi, and T. Takeuchi. 2005. Cytoplasmic transport signal is involved in phogrin targeting and localization to secretory granules. *Traffic.* 6:1213–1224. doi:10.1111/j.1600-0854.2005.00353.x

Turkewitz, A.P. 2004. Out with a bang! *Tetrahymena* as a model system to study secretory granule biogenesis. *Traffic.* 5:63–68. doi:10.1046/j.1600-0854.2003.00155.x

Voets, T., T. Moser, P.E. Lund, R.H. Chow, M. Geppert, T.C. Südhof, and E. Neher. 2001. Intracellular calcium dependence of large dense-core vesicle exocytosis in the absence of synaptotagmin I. *Proc. Natl. Acad. Sci. USA.* 98:11680–11685. doi:10.1073/pnas.201398798

Waites, C.L., A. Mehta, P.K. Tan, G. Thomas, R.H. Edwards, and D.E. Krantz. 2001. An acidic motif retains vesicular monoamine transporter 2 on large dense core vesicles. *J. Cell Biol.* 152:1159–1168. doi:10.1083/jcb.152.6.1159